

Quantum phase transitions in antiferromagnets and superfluids

Subir Sachdev¹ and Matthias Vojta²

Department of Physics, Yale University, P.O. Box 208120, New Haven CT 06520-8120, USA

Abstract

We present a general introduction to the non-zero temperature dynamic and transport properties of low-dimensional systems near a quantum phase transition. Basic results are reviewed in the context of experiments on the spin-ladder compounds, insulating two-dimensional antiferromagnets, and double-layer quantum Hall systems. Recent large N computations on an extended t - J model (cond-mat/9906104) motivate a global scenario of the quantum phases and transitions in the high temperature superconductors, and connections are made to numerous experiments.

Keywords: quantum phase transitions; spin transport; nuclear magnetic resonance; photoemission

1. Introduction

The last decade has seen many experimental studies of the spin dynamics of complex transition metal oxides. Many fascinating new phenomena have been discovered (including high temperature superconductivity), and our understanding of strongly correlated electronic systems has been greatly enhanced. Section 2 of this paper will describe three broad classes of behavior that have been observed in the spin dynamics: many, but not all, of these oxides fall into one of these three classes. We will present this discussion in the context of a description of the zero temperature, quantum phase transition found in a simple, toy model of a two dimensional antiferromagnet of $S = 1/2$ Heisenberg spins. Recent theoretical work on the different non-zero temperature regimes of spin re-

laxation and transport in the vicinity of the quantum phase transition will be described, and correlated with experimental observations.

Related ideas apply also to non-zero temperature *charge* transport in two-dimensional systems in the vicinity of a zero temperature superfluid-insulator transition; these will be briefly noted.

Section 3 of this paper will consider recent theoretical work on the interplay between superconductivity, spin-density-wave and charge-density-wave order in a model of doped two-dimensional antiferromagnets. We will argue that the results suggest a natural scenario under which the transition in the spin sector (from a state with long-range magnetic order to a quantum paramagnet) falls in the same universality class as the simple, undoped insulating model considered in Section 2; this scenario also offers a natural explanation for numerous experiments on the cuprate superconductors. We will also briefly mention charge-ordering transitions in this doped antiferromagnet, and their pos-

¹ E-mail: subir.sachdev@yale.edu

² E-mail: matthias.vojta@yale.edu

sible relationship to the anomalous photoemission linewidths observed in a recent experiment.

We will close in Section 4 by discussing related magnetic transitions in bilayer quantum Hall systems.

2. Coupled ladder antiferromagnet

We will begin our discussion by describing the basic physical properties of a simple quasi two-dimensional model of $S = 1/2$ Heisenberg spins. Our motivation is to introduce essential concepts in the theory of quantum phase transitions [1,2], and to provide a crude picture of the spin fluctuations in the cuprate superconductors—this picture should not be taken too literally though, and a more precise correspondence will be made later in Section 3. Further, there exist insulating transition metal oxides [3] which are described by spin models closely related to the one we consider here.

We consider the Hamiltonian

$$H = J \sum_{i,j \in A} \mathbf{S}_i \cdot \mathbf{S}_j + \lambda J \sum_{i,j \in B} \mathbf{S}_i \cdot \mathbf{S}_j \quad (1)$$

where \mathbf{S}_i are spin-1/2 operators on the sites of the coupled-ladder lattice shown in Fig 1, with the A links forming decoupled two-leg ladders while the B links couple the ladders as shown. The ground state of H depends only on the dimensionless coupling λ , and we will describe the low temperature properties as a function of λ .

For simplicity, we will restrict our attention in this section to the regime $J > 0$, $0 \leq \lambda \leq 1$.

Let us first consider the case where λ is close to 1. Exactly at $\lambda = 1$, H is identical to the square lattice Heisenberg antiferromagnet, and this is known to have long-range, magnetic Néel order in its ground state *i.e.* the spin-rotation symmetry is broken and the spins have a non-zero, staggered, expectation value in the ground state with

$$\langle \mathbf{S}_i \rangle = \eta_i N_0 \mathbf{n}, \quad (2)$$

where \mathbf{n} is some fixed unit vector in spin space, and η_i is ± 1 on the two sublattices. This long-range or-

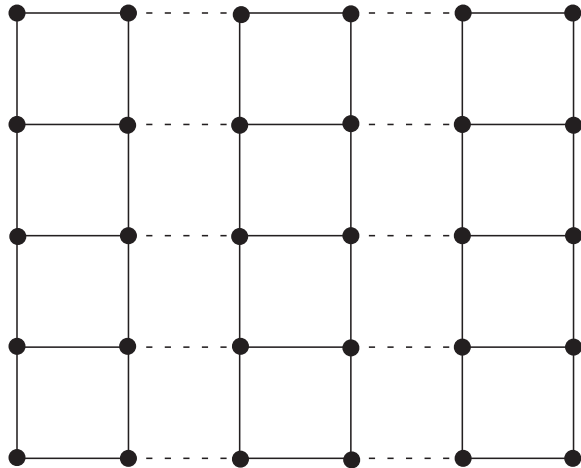


Fig. 1. The coupled ladder antiferromagnet. Spins ($S = 1/2$) are placed on the sites, the A links are shown as full lines, and the B links as dashed lines.

der is expected to be preserved for a finite range of λ close to 1. The low-lying excitations above the ground state consist of slow spatial deformations in the orientation \mathbf{n} in the form of spin waves. There are *two* polarizations of spin waves at each wavevector $k = (k_x, k_y)$ (measured from the antiferromagnetic ordering wavevector), and they have excitation energy $\varepsilon_k = \hbar(c_x^2 k_x^2 + c_y^2 k_y^2)^{1/2}$, with c_x, c_y the spin-wave velocities in the two spatial directions.

Let us turn now to the vicinity of $\lambda = 0$. Exactly at $\lambda = 0$, H is the Hamiltonian of a set of decoupled spin ladders. Such spin ladders are known to have a paramagnetic ground state, with spin rotation symmetry preserved, and an energy gap to all excitations [4]. A caricature of the ground state is sketched in Fig 2: spins on opposite rungs of the ladder pair in valence bond singlets in a manner which preserves all lattice symmetries. Excitations are now formed by breaking a valence bond, which leads to a *three*-fold degenerate state with total spin $S = 1$; this broken bond can hop from site-to-site, leading to a triplet quasiparticle excitation. For λ small, but not exactly 0, we expect that the ground state will remain a gapped paramagnet, and the excited quasiparticle will now move in two dimensions. We parameterize its energy at small

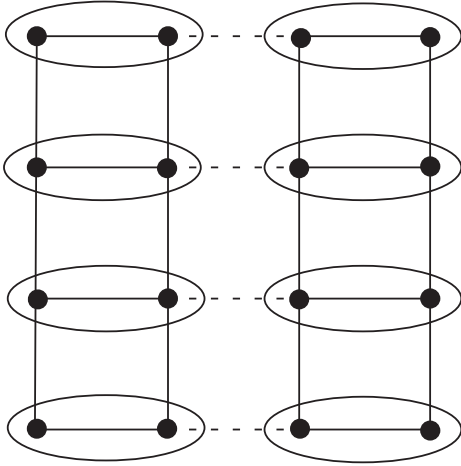


Fig. 2. Schematic of the quantum paramagnet ground state for small λ . The ovals represent singlet valence bond pairs.

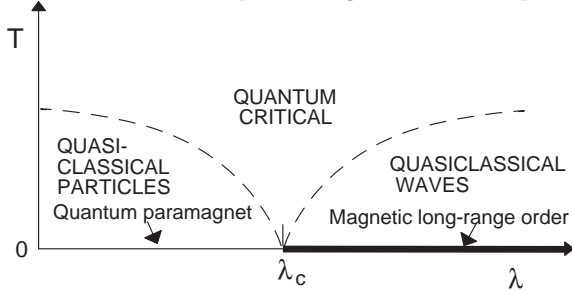


Fig. 3. Phase diagram of H for $T > 0$ and $0 \leq \lambda \leq 1$. The dashed lines represent crossovers.

wavevectors by

$$\varepsilon_k = \Delta + \frac{\hbar^2(c_x^2 k_x^2 + c_y^2 k_y^2)}{2\Delta}, \quad (3)$$

where Δ is the energy gap, and c_x, c_y are velocities.

The very distinct symmetry signatures of the ground states and excitations between $\lambda \approx 1$ and $\lambda \approx 0$ make it clear that the two limits cannot be continuously connected. It is known [5,6] that there is an intermediate second-order phase transition at $\lambda = \lambda_c \approx 0.3$. Both Δ and N_0 vanish continuously as λ_c is approached from either side. The following subsections will consider the distinct physics at very low T for $\lambda > \lambda_c$ and $\lambda < \lambda_c$ respectively (Fig 3). We will find that in both cases a quasiclassical description of the long time dynamics is possible, although the effective classical models are very different. This will be followed by a discus-

sion of the higher temperature ‘quantum critical’ region, where quantum and classical effects are not as easy to disentangle.

2.1. Quasiclassical waves

We consider $\lambda > \lambda_c$, and T very small. This regime was considered in detail in Refs [7].

There are two key observations.

(i) The non-linear interactions between the thermally excited spin waves lead to loss of long-range Néel order at any $T > 0$. The order parameter correlations decay on the scale of the correlation length, ξ , which obeys

$$\xi \sim \exp(2\pi\rho_s/k_B T), \quad (4)$$

where ρ_s is the geometric mean of the spin stiffnesses towards deformations of the ground state in the two directions; a thermodynamic argument shows that $\hbar^2 c_x c_y = \rho_s / \chi_{u\perp}$, where $\chi_{u\perp}$ is the $T = 0$ susceptibility to a uniform magnetic field oriented in a direction orthogonal to the Néel order (both ρ_s and $\chi_{u\perp}$ vanish as $\lambda \searrow \lambda_c$, but c_x, c_y remain finite).

(ii) The most important spin waves occur at a wavevector $k \sim \xi^{-1}$, and at this scale, their thermal occupation number is large:

$$\frac{1}{e^{\varepsilon_k/k_B T} - 1} \gg 1. \quad (5)$$

Consequently, a classical description of these spin wave modes with large occupation numbers is possible.

A continuum Hamiltonian theory of non-linearly interacting waves can be written down in terms of the instantaneous orientation of the Néel order, $\mathbf{n}(x, t)$, and the conserved uniform magnetization density $\mathbf{L}(x, t)$. The $T > 0$ response functions of the antiferromagnet are obtained after integrating over a classical thermal ensemble of initial conditions for \mathbf{n} and \mathbf{L} ; the initial conditions for $\mathbf{L}(x)$ are assumed to be given by a Gaussian with variance controlled by $\chi_{u\perp}$. Note that the allowed values of \mathbf{L} are continuous and there is no signature of quantization of spin—this is a consequence of the

large occupation number of the elementary quantum modes in (5).

A key quantity characterizing the quasiclassical wave dynamics is the phase coherence time τ_φ , loosely defined as the time over which memory of the local orientation of the Néel order parameter is lost. This can be estimated by the equation of motion for \mathbf{n} :

$$\hbar \frac{\partial \mathbf{n}}{\partial t} = \frac{1}{\chi_{u\perp}} \mathbf{L} \times \mathbf{n}, \quad (6)$$

which states that \mathbf{n} precesses about the local magnetization. We can now estimate that

$$\langle |\mathbf{L}| \rangle \sim \sqrt{\langle \mathbf{L}^2 \rangle} \sim \sqrt{k_B T \chi_{u\perp} / \xi^2}, \quad (7)$$

where the last estimate follows from assuming that \mathbf{L} fluctuations have energy $k_B T$ over a scale ξ , and the classical fluctuation-dissipation theorem. From (6) and (7) we may estimate that time over which phase memory is lost is

$$\tau_\varphi \sim \hbar \sqrt{\chi_{u\perp} / k_B T} \xi. \quad (8)$$

This relaxation time controls linewidths in dynamic neutron scattering experiments, and also the relaxation rates in NMR; for the latter we have $1/T_1 \sim \tau_\varphi$, leading to exponentially large values of $1/T_1$ as $T \rightarrow 0$ [8].

2.2. Quasiclassical particles

Now we consider $\lambda < \lambda_c$, and T small.

As argued in Ref [9], a quasiclassical model for the long time dynamics is again possible, but it now involves particles carrying integer quanta of spin, rather than waves with a continuous magnetization. The particles are of course those with excitation energy (3), and at finite T they appear with a density

$$\rho = 3 \int \frac{d^2 k}{4\pi^2} e^{-\varepsilon_k / k_B T} \sim e^{-\Delta / k_B T}. \quad (9)$$

The particles have a kinetic energy of order $k_B T$, and therefore a thermal de-Broglie wavelength of order $1/\sqrt{T}$. So as $T \rightarrow 0$, the particle spacing becomes exponentially large, and eventually exceeds

their de-Broglie wavelength, suggesting that they can be treated classically.

The two-dimensional spin dynamics of these quasi-classical particles can be described in a $1/N$ expansion by a Boltzmann equation [1]. However, for the case where the motion of the particles is quasi one-dimensional *i.e.* for $\lambda = 0$ or with λ small and the observation time shorter than the inter-ladder hopping time, some exact results are possible. We write the magnetization density associated with the thermally activated particles as a sum over particles carrying discrete spin quanta

$$L_z(x, t) = \sum_k m_k \delta(x - x_k(t)), \quad (10)$$

where $x_k(t)$ is the trajectory of particle k which carries azimuthal spin $m_k = 1, 0, -1$ (contrast this with the continuous spin distribution assumed for \mathbf{L} in Section 2.1). The classical Liouville equation for the evolution of the ensemble of $x_k(t)$ can be solved exactly [9,10], and implications for the spin correlations of the underlying antiferromagnet can then be computed, and are described below.

All results in this paragraph are for the case of quasi one-dimensional motion. The interparticle interactions lead to a broadening of the quasi-particle pole in the dynamic structure factor (measured in neutron scattering). This broadening occurs on a time scale, τ_φ , of the order of the time between particle collisions, and this is

$$\tau_\varphi \sim \frac{\hbar}{k_B T} e^{\Delta / k_B T}. \quad (11)$$

The collisions also lead to diffusive transport of spin, and a spin diffusion constant D_s given by

$$D_s = \frac{\hbar c_y^2}{3\Delta} e^{\Delta / k_B T}, \quad (12)$$

where we have assumed that the one-dimensional motion is along the y direction. This diffusive transport can be very clearly detected in NMR experiments [11]. In an external field, H , spin diffusion leads to a $1/\sqrt{H}$ dependence in the $1/T_1$ relaxation rate. The absolute value of $1/T_1$ can also be computed:

$$\frac{1}{T_1} = \frac{\Gamma \Delta e^{-3\Delta/2k_B T}}{c_y^2} \sqrt{\frac{3k_B T}{\pi H}}, \quad (13)$$

where Γ is a hyperfine coupling. The same NMR experiment measuring $1/T_1$ can also detect the uniform susceptibility by the Knight shift, and the present quasiclassical particle model predicts that to be

$$\chi_u = \frac{e^{-\Delta/k_B T}}{\hbar c_y} \sqrt{\frac{2\Delta}{\pi k_B T}}, \quad (14)$$

per unit length of the spin ladder. A striking property of (13,14) is worth emphasizing: note that the $T \rightarrow 0$ activation gap of $1/T_1$ is 3/2 times the activation gap in χ_u . Indeed, this is very close to the experimental trends observed in a large number of quasi one-dimensional spin gap systems, as summarized in Ref [12]. More detailed quantitative comparisons of the theoretical predictions have been performed [10], including the ballistic to diffusive crossover in the particle motion at time scales of order τ_φ , and the agreement with experiments is quite satisfactory.

2.3. Quantum critical dynamics

We now raise the temperature into the quantum critical region, shown in Fig 3.

For $\lambda < \lambda_c$, this region is reached when $k_B T \sim \Delta$. From the arguments above, we see that, for $k_B T \sim \Delta$, the quasiparticle spacing is of order their de-Broglie wavelength, and so a quasiclassical particle picture cannot be generally applicable. Similarly, for $\lambda > \lambda_c$, quantum criticality is reached when $k_B T \sim \rho_s$, and then the occupation number of the important spin-wave modes is of order unity, and a direct quasiclassical wave theory becomes invalid. Thermal and quantum fluctuations are therefore equally important in the quantum critical region, and a simple, intuitive, classical picture of the dynamics does not exist. Rather, progress in our understanding has come from a combination of scaling arguments, and expansions based on $\epsilon = 3 - d$ (d is the spatial dimensionality) and $1/N$ (N is the number of order parameter

components; $N = 3$ for the antiferromagnets being considered here). Further, in some restricted regimes of d , N , or frequency, ω , either a particle or a wave-like picture becomes more appropriate, and further simplifications of the dynamical theory then become possible [1,13,14].

The key property of the quantum-critical regime is that a suitably defined phase coherence time obeys [15,16]

$$\tau_\phi \sim \frac{\hbar}{k_B T}, \quad (15)$$

where the missing proportionality constant is a universal number. This result can be obtained by taking the limiting boundary values of (8,11) as T is raised into the quantum-critical regime. More generally, (15) follows from general scaling arguments, and the fact that $k_B T$ is the most important low energy scale in this regime. This energy scale also controls the value of other observables: the uniform magnetic susceptibility (per unit area) now obeys [17,16]

$$\chi_u = \Omega \frac{k_B T}{\hbar^2 c_x c_y} \quad (16)$$

where Ω is a universal number, and the NMR relaxation rate is given by [17,16]

$$\frac{1}{T_1} \sim T^\eta, \quad (17)$$

where η is an exponent close to 0.

The quantum-critical transport properties are also of some interest. We will express the results in terms of spin conductivity, σ . Unfortunately, it has so far not been possible to measure σ in two-dimensional antiferromagnets, but we hope measurements will appear in the future. However, the properties of *charge* transport near a superfluid-insulator transition of Cooper pairs are very similar, obey the same scaling forms, and are more easily accessible in experiments. The conductivity obeys [18,19]

$$\sigma(\omega, T) = \frac{Q^2}{h} \Sigma \left(\frac{\hbar \omega}{k_B T} \right) \quad (18)$$

where $Q = g\mu_B$ for spin transport and $Q = 2e$ for charge transport, and Σ is a universal scaling function describing the crossover in the dynamical conductivity at a frequency scale of order τ_φ^{-1} . Both $\Sigma(0)$ and $\Sigma(\infty)$ are expected to be finite universal constants, with distinct values. The value $\Sigma(0)$ describes the incoherent d.c. transport in which pre-existing, thermally excited quasiparticles undergo hydrodynamic drift in the applied field; in contrast $\Sigma(\infty)$ describes energy absorbed by pairs of excitations created by an oscillating external field.

3. Doped antiferromagnets

This section will highlight aspects of some recent results [20] on the ground state phase diagram of doped square lattice antiferromagnets. We will focus on the nature of some quantum transitions in the model, their relationship to the simple model we discussed in Section 2, and to experiments on the cuprate superconductors [21].

Ref. [20] considered the phase diagram (Fig 4) of a model of doped antiferromagnets on the square lattice, as functions of the doping δ and a second parameter, N , which can be loosely interpreted as the number of components of each spin. It is also believed that moderately frustrating non-nearest neighbor exchange interactions will have an effect similar to increasing the value of N , and so the vertical axis of Fig 4 can also be considered to be proportional to the strength of such frustration.

The focus in the computation was on the fate of three distinct symmetries of the Hamiltonian in the ground state. There are numerous competing instabilities associated with breaking one or more of these symmetries, and this competition leads to intricate possibilities in the phase diagram. The three symmetries are:

- \mathcal{S} , the electromagnetic $U(1)$ gauge symmetry. This is broken in any superconducting state.
- \mathcal{M} , the $SU(2)$ spin symmetry. This is broken in magnetically ordered states which break spin rotation invariance.

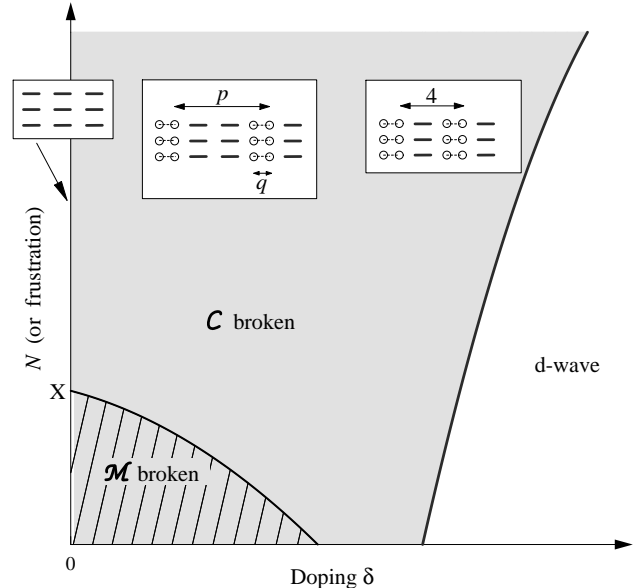


Fig. 4. Ground state phase diagram of a doped antiferromagnet, adapted from Ref [20]. The magnetic \mathcal{M} symmetry is broken in the hatched region, while \mathcal{C} symmetry is broken in the shaded region; there are numerous additional phase transitions at which the detailed nature of the \mathcal{M} or \mathcal{C} symmetry breaking changes - these are not shown. For $\delta = 0$, \mathcal{M} symmetry is broken only below the critical point X , while \mathcal{C} symmetry is broken only above X . The superconducting \mathcal{S} symmetry is broken for all $\delta > 0$ at large N ; for smaller N , the \mathcal{S} can be restored at small δ by additional \mathcal{C} breaking along the vertical axis for the states in the inset—this is not shown. The nature of the \mathcal{C} symmetry breaking at large N is sketched: the thick and dashed lines indicate varying values of the bond charge density, while the circles represent site hole density.

- \mathcal{C} , the symmetry of the space group of the square lattice. We will only consider this broken if an observable invariant under \mathcal{S} and \mathcal{M} does not respect square lattice symmetries. In particular, \mathcal{C} will be broken if the charge density on every bond and site is not identical. Thus the two-sublattice Néel state at $\delta = 0$ breaks only \mathcal{M} while an incommensurate, collinear spin density wave breaks both \mathcal{M} and \mathcal{C} .

An important characteristic of the phases we describe below is that knowledge of the structure of $\mathcal{S}/\mathcal{M}/\mathcal{C}$ breaking gives us essentially complete information on the nature of the ground state and its low energy excitations. In other words, knowing

the symmetry breaking, we can perform a canonical electron Hartree-Fock/BCS small fluctuation analysis, and identify all the important low energy modes. Additional gapless modes with singular interactions and temperature dependencies appear only at quantum critical points between the phases, and these are therefore of central interest.

We first discuss the phases at $\delta = 0$. For small N , the ground state is the two-sublattice Néel state. For larger N , there is a spin-Peierls state with a 2×1 unit cell which breaks \mathcal{C} only (this state has a modulation in the bond charge density). There is evidence [22,1] the transition between these states is second order, and that the \mathcal{M} and \mathcal{C} order parameters vanish continuously as the critical point is approached from opposite sides. It is interesting that a similar phenomenon happens in frustrated spin chains in $d = 1$, where Ising/Néel and spin-Peierls order vanish continuously at the same point and do not co-exist [23]. It appears, therefore, that there is a ‘duality’ between \mathcal{M} and \mathcal{C} order at $\delta = 0$.

Let us now consider non-zero doping $\delta > 0$. One of the key points made in Ref [20] is that it is simpler to first consider doping the spin-Peierls state found at larger N . This has the advantage of ensuring that \mathcal{M} symmetry remains unbroken, and we only have to consider the competition between two symmetries, \mathcal{C} and \mathcal{S} . Such a procedure will be sensible if the \mathcal{C} -ordering instabilities of the cuprate superconductors were, in a sense, more fundamental than the \mathcal{M} -ordering. There is experimental evidence this is the case (the \mathcal{C} -ordering scattering peaks appear at a higher temperature than the \mathcal{M} -ordering) and this supports our approach.

Our results are shown in Fig 4. At low doping one invariably finds one-dimensional striped structures in which the holes are concentrated into regions which are an even number of sites (q) wide. The distance between stripes (p) is inversely proportional to the doping, δ , for small δ , as is found in the cuprate superconductors [21]. The even width is preferred because it promotes the pairing of spins into singlet bonds. This pairing leads to strong superconductivity along the longitudinal stripe di-

rection; there is a weaker Josephson tunneling coupling in the transverse direction, and this eventually leads to two-dimensional superconductivity. Thus the predominant feature of the small $\delta > 0$, and large N , portion of the phase diagram is the co-existence of \mathcal{C} and \mathcal{S} breaking. This co-existence is intrinsically a two-dimensional feature. In one dimension, quasi-long-range charge and superconductivity orders are dual to each other, and do not coexist in a ‘Luther-Emery’ liquid. However, in two dimensions, the additional directional freedom allows coexistence: the charge-density wave ordering is in the x direction, while the superconductivity is predominantly along the longitudinal y direction. At smaller N and small δ , it is possible that additional charge density wave ordering will appear also in the longitudinal direction—we expect the resulting state to then be an insulator. Conversely, at large δ , the \mathcal{C} breaking disappears completely (Fig 4), and we obtain an ordinary d -wave superconductor.

The computation above also allows one to follow the fermionic excitation spectrum in the \mathcal{C} and \mathcal{S} broken phases. In the large doping d -wave superconductor, there are the familiar gapless fermionic excitations at special singular points along the $(1, \pm 1)$ directions. When \mathcal{C} order initially appears (and assuming the absence of time-reversal symmetry breaking), these points move away from the special directions (additional gapless points also appear at image points separated by the new reduced reciprocal lattice vectors). However, when the strength of the \mathcal{C} order is large enough, the gapless points disappear, and the fermion spectrum is gapped over the entire Brillouin zone. Note that at no value of δ is there a sign of a large Fermi surface—instead we have at best gapless Fermi points. This will be crucial in our discussion below of quantum phase transitions.

We now consider the situation at smaller values of N and $\delta > 0$. The most important new physics is the breaking of \mathcal{M} symmetry and the appearance of magnetic order. Unlike the situation at $\delta = 0$, we do not now expect a ‘duality’ between \mathcal{M} and \mathcal{C} order, but expect them to co-exist. This is as in

$d = 1$, where static impurities have been shown to induce a staggered magnetization in \mathcal{C} broken states [24]. The magnetic order is expected in the form of an incommensurate, collinear spin density wave, which breaks both \mathcal{C} and \mathcal{M} symmetries. We expect that the nature of the \mathcal{C} symmetry breaking will not change very much at the $\delta > 0$ transition at which \mathcal{M} symmetry is broken (Fig 4).

3.1. Quantum phase transitions

Let us begin at large δ where the ground state is a d -wave superconductor. Upon decreasing δ we observe two significant quantum phase transitions which we shall discuss further here: the the initial onsets of \mathcal{C} and \mathcal{M} symmetry breaking (Fig 4).

Clearly, the spin/charge-density wave order is the appropriate order parameter for these quantum transitions. In deriving the proper quantum field theory for such an order parameter, the key issue is whether there are any additional low energy excitations which couple efficiently to them. If we were considering the onset of spin/charge-density wave order from a Fermi liquid [25,1], then gapless fermionic excitations at Fermi surface points separated by the ordering wavevector, \mathbf{K} , are key: they lead to a damping of the order parameter modes and determine the universality class of the transition. In the present situation, we have no Fermi surface due to the ubiquity of superconductivity; there are gapless fermionic excitations at isolated points in the Brillouin zone, and so the central issue is whether any pair of these points are separated by a wavevector which equals \mathbf{K} (or its integer multiple) or not.

If the answer to the last question is no, then fluctuations of the spin/charge density order do not scatter fermions between two low lying states; they couple only to short-lived, virtual, fermion particle-hole pair excitations. Such a coupling is quite innocuous and serves only to renormalize the effective couplings in a field theory for the charge/spin density wave order parameter in which the fermionic degrees of freedom have been inte-

grated out. In particular, for the onset of \mathcal{M} symmetry breaking, the form of the effective action will be identical to that for the quantum phase transition in the coupled ladder model studied in Section 2. In this case, most of the results in the distinct dynamical regimes of Sections 2.1, 2.2, and 2.3 can be applied essentially unchanged to the present model. Related results will also hold for the onset of \mathcal{C} order.

In contrast, if \mathbf{K} does equal the distance between two gapless Fermi points, a somewhat different situation obtains. Now a theory of order parameter modes coupled with the gapless fermion excitations is necessary. A theory of this type has been studied recently by Balents *et al* [26], who consider the onset of \mathcal{M} ordering in a d -wave superconductor. A related model for \mathcal{C} ordering was proposed in Ref [20]. These theories are expected to possess a quantum scale-invariant critical point with the exponent η not necessarily close to 0. However, general features of the finite temperature crossovers are expected to be similar to those in Section 2.

3.2. Implications for cuprate superconductors

First, let us consider the \mathcal{M} ordering transition. There are a number of experiments in $\text{La}_{2-x}\text{Sr}_x\text{CuO}_4$ which are consistent with the interpretation that such a transition, with collinear incommensurate magnetic order, happens at around $x \approx 0.11$.

- The early NMR measurements of Imai *et al* examined the T dependence of $1/T_1$ for a variety of values of x ; their measurements neatly fall into the three classes of behavior discussed in Sections 2.1, 2.2, and 2.3, with the last being consistent with an $\eta \approx 0$. More recent NQR measurements [28] are sensitive to charge order, and are consistent with the topology of the phase diagram sketched in Fig 4.
- The neutron scattering measurements of Aeppli *et al* [29], as well as earlier work [30,31], indicate quantum critical scaling in the dynamic spin structure factor with dynamic exponent $z \approx 1$

and $\eta \approx 0$.

- Recent NMR measurements of the transverse relaxation time, T_2 [32], also indicate $z = 1$ criticality.
- Numerous neutron scattering experiments [33–36] have observed a sharp, high energy ‘resonance peak’ near the antiferromagnetic ordering wavevector. Although a momentum-dependent dispersion of this peak has not (yet) been observed, it is tempting to identify it with the quasiclassical particles of Section 2.2.

We turn next to the onset of \mathcal{C} order. There are no direct signatures yet of critical fluctuations associated with such a transition [37]. However, it has been proposed in Ref [20] that the anomalous momentum linewidths observed in a recent photoemission [38] experiment could be due to the scattering of the fermions from critical \mathcal{C} order fluctuations, as obtains in the theory discussed in the latter part of Section 3.1.

4. Quantum Hall bilayers

In closing, we briefly mention another experimental system in which magnetic ordering transitions appear to have been observed; in this case, a number of experimental knobs can rather easily tune the parameters in the Hamiltonian, and the prospects from more detailed experimental studies are good.

The transitions have been observed in a bilayer quantum Hall system at filling fraction $\nu = 2$ [39,40]. The electrons in each layer occupy a fully filled Landau level at $\nu = 1$, and so it is not unreasonable in a first study to focus simply on the spin degrees of freedom. Indeed, a reasonable caricature of the physics can be obtained by imagining that the electrons are rigidly fixed on equivalent lattices in each layer, and by describing their interactions with an insulating spin model, as in (1); such a model has ferromagnetic exchange interaction within each layer (*i.e.* the links in set A in (1) couple nearest neighbor sites within each layer

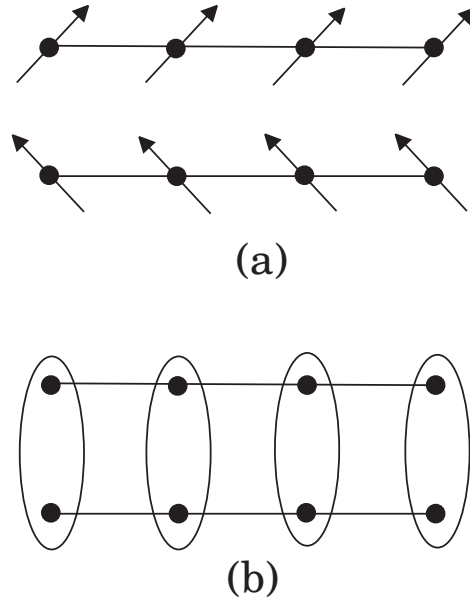


Fig. 5. Schematic of the distinct ground states in the double layer quantum Hall system at $\nu = 2$; the state (a) is magnetically ordered, while (b) is a spin-singlet quantum paramagnet.

and have $J < 0$), and antiferromagnetic exchange between the layers (the links in set B couple the two layers and have $\lambda J > 0$). The limiting ground states of such a Hamiltonian can now be understood in manner similar to the discussion in Section 2, and are sketched in Fig 5; for large $|\lambda|$ the ground state is a quantum paramagnet in which the spins in opposite layers pair to form singlets, while magnetically ordered states are present at small λ . A number of theoretical studies [41–49] of such spin models, and others which include the orbital motion in the Landau levels, have appeared, and a quantitative confrontation between theory and experiment should be possible in the future.

Acknowledgement

We thank Kedar Damle, Sankar Das Sarma, Robert Laughlin, Jan Zaanen, and Shoucheng Zhang for useful discussions and collaborations. This research was supported by US NSF Grant No DMR 96–23181 and by the DFG (VO 794/1-1).

References

- [1] S. Sachdev, *Quantum Phase Transitions*, Cambridge University Press, Cambridge (1999).
- [2] S. Sachdev, *Physics World*, **12**, No. 4, 33 (1999).
- [3] M. Azuma, Z. Hiroi, M. Takano, K. Ishida, and Y. Kitaoka *Phys. Rev. Lett.* **73**, 3463 (1994).
- [4] E. Dagotto and T. M. Rice, *Science* **271**, 618 (1996).
- [5] N. Katoh and M. Imada, *J. Phys. Soc. Jpn.* **63**, 4529 (1994).
- [6] J. Tworzydło, O. Y. Osman, C. N. A. van Duin, and J. Zaanen, *Phys. Rev. B* **59**, 115 (1999).
- [7] S. Chakravarty, B. I. Halperin, and D. R. Nelson, *Phys. Rev. B* **39**, 2344 (1989); S. Tyc, B. I. Halperin, and S. Chakravarty, *Phys. Rev. Lett.* **62**, 835 (1989).
- [8] S. Chakravarty and R. Orbach, *Phys. Rev. Lett.* **64**, 224 (1990).
- [9] S. Sachdev and K. Damle, *Phys. Rev. Lett.* **78**, 943 (1997).
- [10] K. Damle and S. Sachdev, *Phys. Rev. B* **57**, 8307 (1998).
- [11] M. Takigawa, T. Asano, Y. Ajiro, M. Mekata, and Y. J. Uemura, *Phys. Rev. Lett.* **76**, 2173 (1996).
- [12] Y. Itoh and H. Yasuoka, *J. Phys. Soc. Jpn.* **66**, 334 (1997).
- [13] S. Sachdev, *Phys. Rev. B* **59**, 14054 (1999).
- [14] S. Sachdev and O. A. Starykh, *cond-mat/9904354*.
- [15] S. Sachdev and J. Ye, *Phys. Rev. Lett.* **69**, 2411 (1992).
- [16] A. V. Chubukov, S. Sachdev, and J. Ye, *Phys. Rev. B* **49**, 11919 (1994).
- [17] A. V. Chubukov and S. Sachdev, *Phys. Rev. Lett.* **71**, 169 (1993).
- [18] K. Damle and S. Sachdev, *Phys. Rev. B* **56**, 8714 (1997).
- [19] M. P. A. Fisher, G. Grinstein, and S. M. Girvin, *Phys. Rev. Lett.* **64**, 587 (1990).
- [20] M. Vojta and S. Sachdev, *cond-mat/9906104*.
- [21] For a review of previous work on charge and spin ordering in the cuprate superconductors see V. J. Emery, S. A. Kivelson, and J. M. Tranquada, *cond-mat/9907228*, and S. Caprara, C. Castellani, C. Di Castro, M. Grilli, and A. Perali, *cond-mat/9907265* and references therein.
- [22] V. N. Kotov, J. Oitmaa, O. P. Sushkov, and W. Zheng, *cond-mat/9903154*; R. R. P. Singh, W. Zheng, C. J. Hamer, and J. Oitmaa, *cond-mat/9904064*; V. N. Kotov and O. P. Sushkov, *cond-mat/9907178*; O. P. Sushkov, *cond-mat/9907400*.
- [23] F. D. M. Haldane, *Phys. Rev. B* **25**, 4925 (1982).
- [24] H. Fukuyama, T. Tanimoto, and M. Saito, *J. Phys. Soc. Jpn.* **65**, 1182 (1996); M. Fabrizio and R. Mélin, *Phys. Rev. B* **56**, 5996 (1997); M. Mostovoy, D. Khomskii, and J. Knoester, *Phys. Rev. B* **58**, 8190 (1998).
- [25] J. A. Hertz, *Phys. Rev. B* **14**, 1165 (1976).
- [26] L. Balents, M. P. A. Fisher, and C. Nayak, *Int. J. Mod. Phys. B* **12**, 1033 (1998).
- [27] T. Imai, C. P. Slichter, K. Yoshimura, K. Kosuge, *Phys. Rev. Lett.* **70**, 1002 (1993); T. Imai, C. P. Slichter, K. Yoshimura, M. Katoh, and K. Kosuge, *Phys. Rev. Lett.* **71**, 1254 (1993).
- [28] A. W. Hunt, P. M. Singer, K. R. Thurber, and T. Imai, *Phys. Rev. Lett.* **82**, 4300 (1999).
- [29] G. Aeppli, T. E. Mason, S. M. Hayden, H. A. Mook, and J. Kulda, *Science* **278**, 1432 (1997).
- [30] S. M. Hayden, G. Aeppli, H. Mook, D. Rytz, M. F. Hundley, and Z. Fisk, *Phys. Rev. Lett.* **66**, 821 (1991).
- [31] B. Keimer, N. Belk, R. J. Birgeneau, A. Cassanho, C. Y. Chen, M. Greven, M. A. Kastner, A. Aharony, Y. Endoh, R. W. Erwin, and G. Shirane, *Phys. Rev. B* **46**, 14034 (1992).
- [32] S. Fujiyama, M. Takigawa, Y. Ueda, T. Suzuki, and N. Yamada, *cond-mat/9904275*.
- [33] J. Rossat-Mignod, L. P. Regnault, C. Vettier, P. Bourges, P. Bulet, J. Bossy, J. Y. Henry, and G. Lapertot, *Physica C* **185-189**, 86 (1991).
- [34] H. A. Mook, M. Yehiraj, G. Aeppli, T. E. Mason, and T. Armstrong, *Phys. Rev. Lett.* **70**, 3490 (1993).
- [35] H. F. Fong, B. Keimer, F. Dogan, and I. A. Aksay, *Phys. Rev. Lett.* **78**, 713 (1997).
- [36] P. Bourges in *The Gap Symmetry and Fluctuations in High Temperature Superconductors* ed. J. Bok, G. Deutscher, D. Pavuna, and S. A. Wolf (Plenum, New York, 1998); *cond-mat/9901333*.
- [37] However, indirect experimental signatures for a somewhat different C ordering transition (of the type in Ref. [25]) have been claimed by Caprara *et al* [21].
- [38] T. Valla, A. V. Fedorov, P. D. Johnson, B. O. Wells, S. L. Hulbert, Q. Li, G. D. Gu, and N. Koshizuka, *Brookhaven preprint* (1999).
- [39] V. Pellegrini, A. Pinczuk, B. S. Dennis, A. S. Plaut, L. N. Pfeiffer, and K. W. West, *Phys. Rev. Lett.* **78**, 310 (1997); *Science* **281**, 799 (1998).
- [40] A. Sawada, Z. F. Ezawa, H. Ohno, Y. Horikoshi, Y. Ohno, S. Kishimoto, F. Matsukura, M. Yasumoto, A. Urayama, *Phys. Rev. Lett.* **80**, 4534 (1998).
- [41] L. Zheng, R. J. Radtke, and S. Das Sarma, *Phys. Rev. Lett.* **78**, 2453 (1997).

- [42] S. Das Sarma, S. Sachdev, and L. Zheng, Phys. Rev. Lett. **79**, 917 (1997).
- [43] S. Das Sarma, S. Sachdev, and L. Zheng, Phys. Rev. B **58**, 4672 (1998).
- [44] M. Troyer and S. Sachdev, Phys. Rev. Lett. **81**, 5418 (1998).
- [45] Z.F. Ezawa, Phys. Rev. Lett. **82**, 3512 (1999).
- [46] E. Demler and S. Das Sarma, Phys. Rev. Lett. **82**, 3895 (1999).
- [47] L. Brey, E. Demler, and S. Das Sarma, Phys. Rev. Lett. **83**, 168 (1999).
- [48] A. H. MacDonald, R. Rajaraman, and T. Jungwirth, cond-mat/9903318.
- [49] E. Demler, E. H. Kim, and S. Das Sarma, cond-mat/9907107.